SENSITIVITY OF SIMULATED WATER ABSORPTION CHARACTERISTICS TO EMPIRICAL HYDRAULIC DIFFUSIVITY MODELS FOR POROUS BUILDING MATERIALS

Korakuti Hanumanthu[1], Kaustav Sarkar[1]

1. School of Engineering, IIT Mandi, Himachal Pradesh, India

ABSTRACT. The phenomena of water absorption in porous building materials have been conventionally represented using a parabolic partial differential equation with hydraulic diffusivity as the transport parameter. The equation in its linear and non-linear forms has been widely adopted in the modeling of hydraulic diffusivity in terms of water absorption coefficient and other non-linear functions of moisture content based on pertinent experimental data. The objective of this paper is to assess the sensitivity of moisture intrusion characteristics, namely, (i) the moisture content and, (ii) the moisture penetration depth, to different hydraulic diffusivity models. The stated characteristics have been simulated with a duly verified Crank- Nicolson scheme modified to reduce computational cost related to the iterative solution. The scope of the study includes the cases of two distinct materials – fired clay brick and OPC-lime-sand mortar – for which experimentally observed moisture intrusion profiles are available from independently reported studies. The simulated moisture profiles are observed to remain concave upwards initially and become linear at later stages in cases where the governing model is linear. Although this pattern closely conforms to the trigonometrical series solution for the model, it does not match the experimentally observed distribution. It is observed that the non-linear model provides better estimates of moisture intrusion characteristics. The moisture dependent diffusivity value matches the magnitude of constant diffusivity only at a near saturation condition. The study further reveals that, that the non-linear model performs better in the case of fired clay brick than for OPC-lime-sand mortar.

Keywords: Porous building materials, Hydraulic diffusivity, FDM, Water absorption coefficient.

Mr Korakuti Hanumanthu is a Ph.D. research scholar in School of Engineering at IIT Mandi. His area of interest is the modeling and simulation of water transport in porous building materials.Telephone: +917807123690 Email Id: d16030@students.iitmandi.ac.in

Dr Kaustav Sarkar is an Assistant Professor in the School of Engineering at IIT Mandi. His areas of research interest include computational modeling of the transport process in concrete, soft computing, optimum design, and sustainable concrete production.
Telephone with Country Code: +918628978584 Email Id: srkr@iitmandi.ac.in

INTRODUCTION

Moisture plays a critical role in many degradation processes affecting porous building materials. Changes in moisture levels can cause damages, such as decoloration, cracking, chipping and disintegration etc. Moisture can enter into the porous matrix in liquid and/or vapor form. The capillary absorption of liquid water in porous building materials is known to occur at a faster rate than the vapor diffusion process [1]. Water absorption can occur under various exposure conditions, e.g. due to the action of driving rain, runoff from roof and façade, and the capillary rise of groundwater etc. [2]. The need to render building components durable requires making them adequately impervious to water absorption. While the degree of water tightness of a material can be determined directly through standard water absorption and permeation tests, the estimation of the service life of a building component requires the modeling and simulation of water absorption under the given conditions of service [3, 4 and 5].

Capillary absorption of water is known to rely upon the initial state of saturation and temperature conditions [4]. The quantity and penetration depth of absorbed water remains constant for initial saturation levels of up to about 20% RH, thereafter these values increase until the range of 75-80% RH and steadily decrease towards zero due to the self-sealing effect of the hydrated gel at about 90% RH and above [5]. The effect of the temperature, on the other hand, becomes significant only under non-isothermal conditions [6]. Under isothermal conditions, the water absorption coefficient and hydraulic diffusivity remain practically constant in relation to the temperature of water for brick and concrete but exhibit a linear relationship in the case of eastern white pine [7 and 8].

The study of one-dimensional capillary water absorption in porous building materials is carried out using standard methods involving gravimetric measurement. The measured data is used to quantify parameters, such as sorptivity and water absorption coefficient [9 and 10]. These parameters facilitate the relative comparison of the potential durability of one material with respect to the other [11]. These parameters have also been used to model hydraulic diffusivity either as a constant or as a function of moisture content. Typically, constant hydraulic diffusivity values are calculated using the water absorption coefficient (equations 4 and 5) and the moisture dependent hydraulic diffusivity function is stated in terms of sorptivity [12]. The modelling of hydraulic diffusivity as a function of moisture content also requires the estimation of water absorption profiles either by means of non-destructive measurement, such as Nuclear Magnetic Resonance (NMR) [13], Gamma-ray and X-ray attenuation [14], Time Domain Reflectometry [15] etc. or through the implementation of assumed models fitted using gravimetric measurements [16].

The present study aims to evaluate the sensitivity of the simulated moisture intrusion characteristics namely, (i) the moisture content and, (ii) the moisture penetration depth to linear and non-linear governing models using appropriate forms of Crank- Nicolson finite difference scheme. The study considers the cases of two distinct materials –fired clay brick and OPC-lime-sand mortar- for which experimentally observed moisture intrusion profiles have been previously reported [17 and 18]. The developed linear model has been verified using closed form analytical solutions stated in terms of error function and trigonometrical series. Observations reveal that the simulated moisture profiles match closely to the pattern defined by trigonometrical series solution. The profiles obtained with the linear model are initially concave upwards and tend to become linear at later time levels. This pattern does not match the experimental observations. The results affirm the suitability of a non-linear governing model on the aspects of the shape of simulated moisture distribution, moisture content and penetration depth. The study also reveals that the non-linear model performs better in the case of fired clay brick than for OPC-lime-sand mortar.

MODELING OF WATER ABSORPTION IN UNSATURATED POROUS MATERIALS

Linear Governing Equation

One-dimensional water absorption in porous building materials is described by the partial parabolic differential equation [19 and 20]:

$$\frac{\partial \theta}{\partial t} = D' \frac{\partial^2 \theta}{\partial x^2} \tag{1}$$

where θ (m^3/m^3) is the volumetric moisture content, t (s) is time, x (m) is spatial distance and D' (m^2/s) is the hydraulic diffusivity. Equation (1) becomes linear if $D' = D$ is constant and non-linear when $D' = D(\theta)$ is considered to be moisture dependent. The solution to equation (1) requires the specification of one initial condition and two boundary conditions.

A closed form solution for initial time levels to the linear form of equation (1) is stated as [19, 20, 21]:

$$\theta_n(t,x) = \left[1 - erf\left(\frac{x}{\sqrt{4Dt}}\right)\right] \tag{2}$$

The solution expressed in equation (2) is valid under the following assumptions:
The medium is initially dry i.e. $\theta(t = 0, 0 < x < \infty) = 0$
The boundary points are subjected to a constant moisture level i.e. $\theta(t \geq 0, x = 0) = 1$ and $\theta(t \geq 0, x = \infty) = 0$.

Another closed form solution to the equation (1) for later time levels is stated as [19]:

$$\theta_n(t,x) = \theta(t,0) + \left(\theta(t,L) - \theta(t,0)\right)\frac{x}{L} + \frac{2}{\pi}\sum_{n=1}^{\infty}\frac{\theta(t,L)\cos n\pi - \theta(t,0)}{n}\sin\frac{n\pi x}{L}\exp\left(\frac{-Dn^2\pi^2 t}{L^2}\right)$$
$$+\frac{4\theta(0,x)}{\pi}\sum_{m=0}^{\infty}\frac{1}{2m+1}\sin\frac{(2m+1)\pi x}{L}\exp\left\{-D(2m+1)^2\pi^2 t/L^2\right\} \tag{3}$$

The solution expressed in equation (3) is valid under the following assumptions:
The medium is initially dry i.e. $\theta(t = 0, 0 < x < L) = 0$
The boundary points are subjected to a constant moisture level i.e. $\theta(t \geq 0, x = 0) = 1$ and $\theta(t \geq 0, x = L) = 0$.
The closed form solutions given by equations (2) and (3) has been subsequently used in this work to verify the finite difference scheme constituted to simulate the moisture distribution

and moisture content. Constant values for D (m^2/s) have been determined using equations (4) and (5) based on the water absorption coefficient [22].

$$D \approx \left(A / \theta_s \right)^2 \tag{4}$$

$$D = \pi / 4 \left(A / \theta_s \right)^2 \tag{5}$$

where θ_s (m^3/m^3) is the saturation moisture content and A [$kg/(m^2 \sqrt{s})$] is the water absorption coefficient given by [11 and 23]:

$$A = m_w(t) / a\sqrt{t} \tag{6}$$

where, $m_w(t)$ (kg) is the cumulative water uptake at time t, a (m^2) is the surface area exposed to water and t (s) is the time.

Normalized Governing Equation

The normalization of variables in equation (1) becomes necessary to minimize computational errors and thus the following normalized variables were adopted [24]:

Normalized water content, $\theta_n = (\theta - \theta_{\min}) / (\theta_{\max} - \theta_{\min})$ (7a)

Normalized space variable, $x_n = x/L$ (7b)

Normalized time variable for $D' = D$, $t_n = \left(D/L^2 \right) t$ (7c)

where, $\theta_{\min}$ (m^3/m^3) is the minimum moisture content and is equal to zero for an initially dry state, $\theta_{\max}$ (m^3/m^3) is the moisture content at the saturated state and L (m) is the length of specimen Using (7a-7c), equation (1) can be restated as:

$$\frac{\partial \theta_n}{\partial t_n} = \frac{\partial^2 \theta_n}{\partial {x_n}^2} \tag{8}$$

If the governing model is taken to be non-linear with:

$$D' = D(\theta) = D_0 \exp(n\theta) \tag{9}$$

where D_0 is the diffusivity at dry state and n is the shape parameter, which range is 6-8 for different building materials [2], then, the normalized time variable, $t_n = \left(D_0 / L^2 \right) t$. The normalized governing equation for this case can be stated as:

$$\frac{\partial \theta_n}{\partial t_n} = \frac{\partial}{\partial x_n} \left(\exp\left(n \theta_{\max} \theta_n \right) \right) \frac{\partial \theta_n}{\partial x_n} \tag{10}$$

Finite Difference Formulation

Applying the Crank-Nicolson scheme to equation (8):

$$\frac{\theta_n^{i,j+1}-\theta_n^{i,j}}{k}=\frac{1}{2}\left(\frac{\theta_n^{i+1,j+1}-2\theta_n^{i,j+1}+\theta_n^{i-1,j+1}}{h^2}+\frac{\theta_n^{i+1,j}-2\theta_n^{i,j}+\theta_n^{i-1,j}}{h^2}\right)$$

where the superscripts *i* and *j* denote the node and time step numbers respectively, *h* is the element length and *k* is the time step size respectively. Separating the j^{th} and $(j+1)^{th}$ terms to the right and left sides of the equation:

$$\frac{-r}{2}\theta_n^{i+1,j+1}+\left(1+r\right)\theta_n^{i,j+1}-\frac{r}{2}\theta_n^{i-1,j+1}=\frac{r}{2}\theta_n^{i+1,j}+\left(1-r\right)\theta_n^{i,j}+\frac{r}{2}\theta_n^{i-1,j} \tag{11}$$

Here, $r = k/h^2$

Applying a modified Crank-Nicolson scheme [25] to equation (10):

$$\frac{\theta_n^{i,j+1}-\theta_n^{i,j}}{k}=\left[\left(D_n\right)\frac{\partial\theta_n}{\partial x_n}\Big|_{i+1,j}-\left(D_n\right)\frac{\partial\theta_n}{\partial x_n}\Big|_{i,j}+\left(D_n\right)\frac{\partial\theta_n}{\partial x_n}\Big|_{i+1,j+1}-\left(D_n\right)\frac{\partial\theta_n}{\partial x_n}\Big|_{i,j+1}\right]\frac{1}{2h}$$

where, $D_n=\exp\left(n\theta_{\max}\theta_n\right)$ and other notations have usual meanings. Separating the terms pertaining to j^{th} and $(j+1)^{th}$ time steps to the right and left sides of the equation:

$$\begin{aligned}&-\left(0.5r\left(D_n\right)_{i-1/2}\right)\theta_n^{i-1,j+1}+\left(1+0.5r\left(\left(D_n\right)_{i+1/2}+\left(D_n\right)_{i-1/2}\right)\right)\theta_n^{i,j+1}-\left(0.5r\left(D_n\right)_{i+1/2}\right)\theta_n^{i+1,j+1}=\\&\left(0.5r\left(D_n\right)_{i-1/2}\right)\theta_n^{i-1,j}+\left(1-0.5r\left(\left(D_n\right)_{i+1/2}+\left(D_n\right)_{i-1/2}\right)\right)\theta_n^{i,j}+\left(0.5r\left(D_n\right)_{i+1/2}\right)\theta_n^{i+1,j}\end{aligned} \tag{12}$$

Here, $r = k/h^2$; $\left(D_n\right)_{i+1/2}=0.5\left(\left(D_n\right)_i+\left(D_n\right)_{i+1}\right)$ and $\left(D_n\right)_{i-1/2}=0.5\left(\left(D_n\right)_i+\left(D_n\right)_{i-1}\right)$

Equations (11) and (12) provide the moisture distribution at $(j+1)^{th}$ time level using the j^{th} time level values. Specifically in the case of equation (12), the $(D_n)_{i\pm 1/2}$ values corresponding to the $(j+1)^{th}$ time level are substituted with the corresponding values for the j^{th} time level. This procedure is used to avoid the necessity of having sub iterations. The approach has been referred to as the modified Crank-Nicolson method in literature and is known to produce reliable results [25]. The solution procedure produces a set of linear simultaneous equations of tridiagonal form which can be effectively handled using the Thomas algorithm. A C++ program was created to implement the numerical scheme with the following initial and boundary conditions to simulate the water absorption phenomena:

- $\theta_n = 0$, for $0 \le x_n \le 1$ at $t_n = 0$
- $\theta_n = 1$, at $x_n = 0$, and $t_n > 0$
- $\theta_n = 0$, at $x_n = 1$, and $t_n > 0$

RESULTS AND DISCUSSIONS

The scope of this study is to evaluate the sensitivity of the simulated moisture intrusion characteristics namely, (i) the moisture content and, (ii) the moisture penetration depth to linear and non-linear governing models using appropriate forms of Crank- Nicolson finite difference scheme for fired clay brick and OPC-lime-sand mortar. Experimental data of moisture distribution profiles for the considered materials were extracted from previously reported studies [17 and 18]. In both, the cases moisture distribution profiles were measured using Nuclear Magnetic Resonance (NMR) and consequently the moisture dependent hydraulic diffusivity was modeled through inverse analysis using Boltzmann's transformation. Relevant details of experimentation and material properties have been summarized in Table 1.

Table 1 Data on water absorption test

MATERIAL	FIRED CLAY BRICK	OPC-LIME-SAND MORTAR
Moisture profiles	4, 9, 15, 27, 34 and 47 minutes	38, 57, 97, 208 and 271 minutes
θ_s (m^3/m^3)	0.265	0.27
L (m)	0.1	0.235
Temperature (^{o} C)	20	19.85 (293 ± 0.5 K)
A [$kg/(m^2 \sqrt{s})$]	0.40	0.27
D (m^2/s) $(eq\ 4)$	2.15 X 10^{-06}	9.99 X 10^{-07}
D (m^2/s) $(eq\ 5)$	1.69 X 10^{-06}	7.84 X 10^{-07}
D_o (m^2/s)	4.2 X 10^{-09}	8.2 X 10^{-09}
N	*7.56*	*6.55*

The reliability of the developed numerical scheme has been verified by comparing the results obtained from equation (11) with those determined with the closed form solution in equations (2) and (3) at each time level. The comparison has been carried out in terms of moisture content calculated as the area under the individual curves using trapezoidal rule. The plot of absolute percentage difference of moisture content derived from equations (2) and (3) with respect to the simulated results corresponding to the cases of constant hydraulic diffusivity given by equations (4) and (5) have been illustrated in Figures 1 and 2 for fired clay brick and OPC-lime-sand mortar respectively.

It is clearly evident that the simulations exhibit a close match to the trigonometrical series of equation (3). On the other hand, the differences with respect to the error function solution of equation (2) are conspicuously larger than the previous case and tend to increase with increasing time. The results obtained with hydraulic diffusivity determined as per equation (5) are better than those obtained with equation (4) in case of the error function solution. This effect is however negligible in case of trigonometrical series solution.

Figures 3 and 4 illustrate the moisture distribution profiles corresponding to individual time levels for the cases of fired clay brick and OPC-lime-sand mortar respectively obtained with hydraulic diffusivity as per equation (5). The plots exhibit the close conformity of simulated results to those obtained with trigonometrical series solution. The moisture profiles are initially concave upwards and tend to become linear at later time levels. However, this pattern does not match the experimentally observed profiles as shown in Figures 5 and 6. Hence, the study has been extended to the case of non-linear models as described in the following paragraphs.

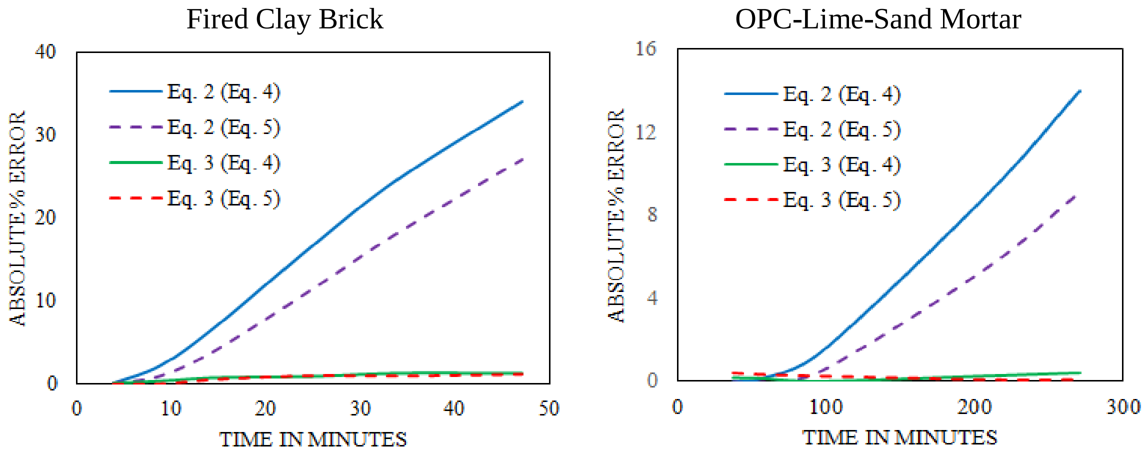

Figures 1 and 2 Absolute % error vs Time

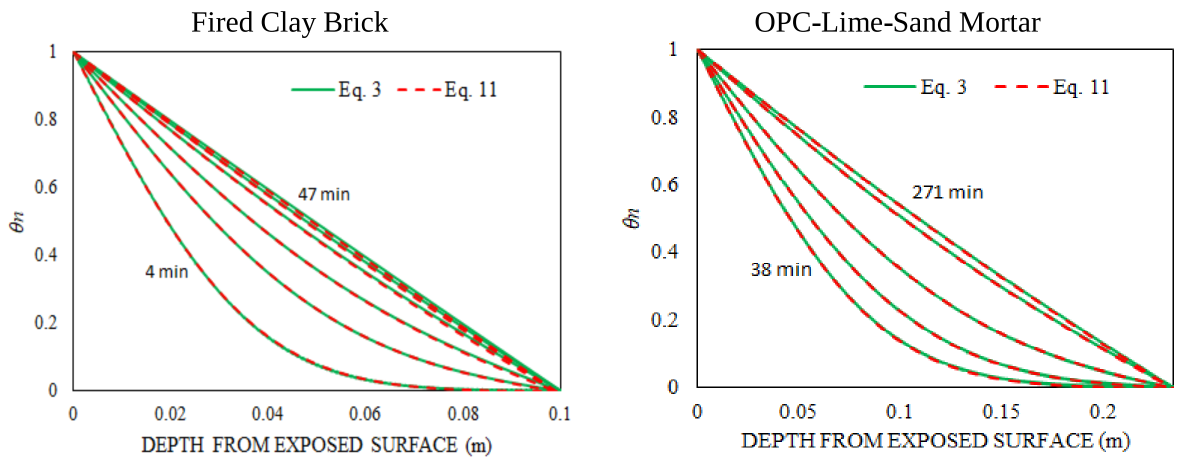

Figures 3 and 4 Trigonometrical series solution vs FDM results for linear diffusion model for fired clay brick at 4, 9, 15, 25, 34 and 47 minutes and OPC-lime-sand mortar at 38, 57, 97, 208 and 271 minutes.

The moisture profiles furnished in Figures 5 and 6 have been simulated with the exponential diffusivity function given in equation (9) using the modified Crank-Nicolson scheme stated in equation (12). The simulated moisture distribution plots exhibit a close match on the aspects of the shape, moisture content and penetration depth, hence, validating the suitability of the non-linear governing model. The estimates of absolute percentage difference in moisture content and penetration depth have been calculated with respect to the experimental data and are given in Table 2. It is evident that, the non-linear governing model has performed better in the case of fired clay brick than for the OPC-lime-sand mortar. These observations affirm the anomalous water absorption trait of the mortar specimen which is known to manifest due to the swelling of the gel phase and consequent redistribution of capillary and gel pore spaces. The observation also connotes to the inadequacy of the Boltzmann's transformation approach to the modeling of hydraulic diffusivity. The average of absolute differences was therefore a bit on the higher side at 18.92% in this case.

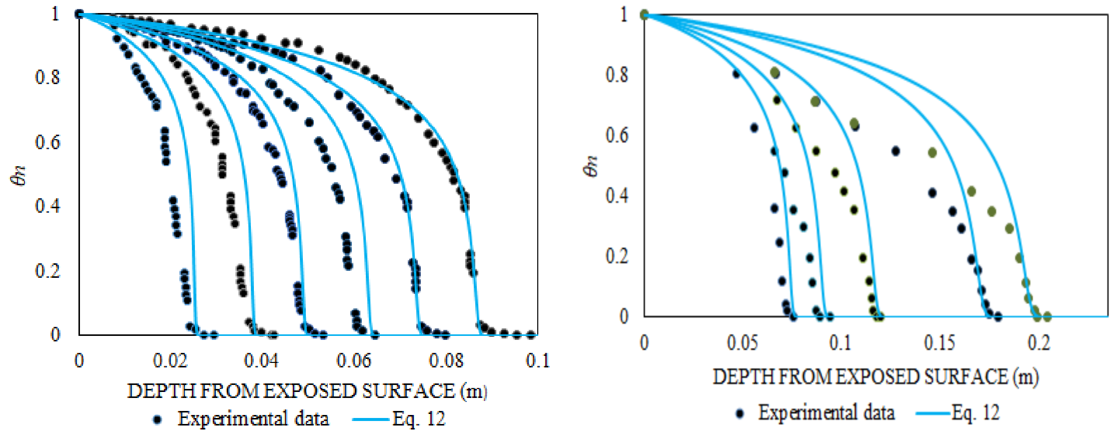

Figures 5 and 6 Simulated vs observed moisture profiles for fired clay brick at 4, 9, 15, 25, 34 and 47 minutes and OPC-lime-sand mortar at 38, 57, 97, 208 and 271 minutes.

Table 2 Error in simulated data with respect to experimental observations for fired clay brick and OPC-lime-sand-mortar

CONTENTS	FIRED CLAY BRICK	OPC-LIME-SAND-MORTAR
Average Absolute Percentage Error of Moisture Content	3.65 %	18.92 %
Average Absolute Percentage Error of Penetration Depth	6.76 %	9.60 %

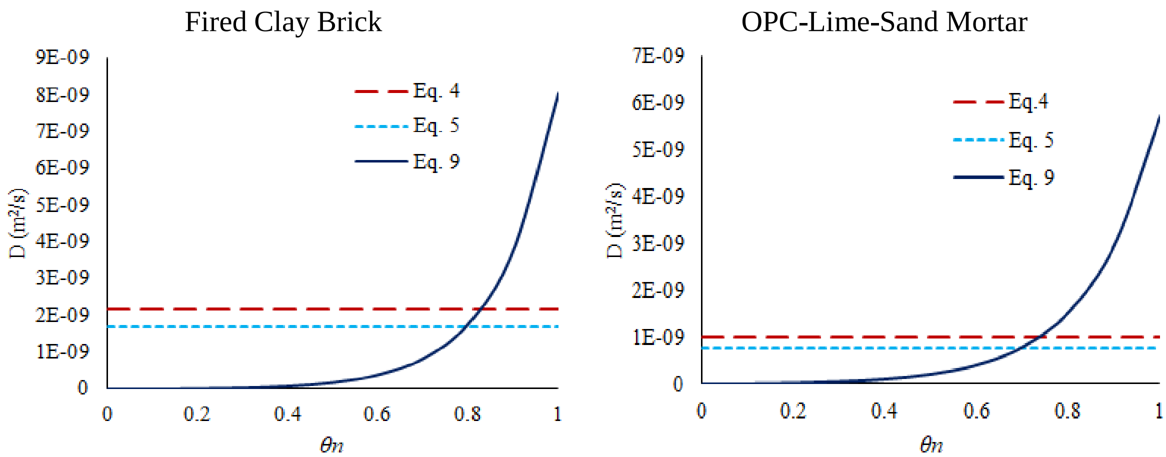

Figures 7 and 8 Hydraulic diffusivity vs normalized moisture content

Figures 7 and 8 highlight the variation of hydraulic diffusivity as a function of normalized moisture content. It can be discerned from the plot that constant hydraulic diffusivity values corresponding to equations (4) and (5) equal the magnitude of moisture dependent hydraulic diffusivity given by equation (9) at saturation levels of about 80% and 70% for fired clay brick and OPC-lime-sand mortar respectively. This would in turn lead to an over estimation at lower and under estimation at higher saturation levels when using a linear model for the simulation of moisture intrusion characteristics.

CONCLUSIONS

This study reaffirms the suitability of the non-linear governing model for the simulation of water absorption in porous building materials. Nevertheless, the linear models provide a convenient means to verify a numerical scheme due to the availability of closed form solutions. The observations made in this study are summarized as under:

1. The trigonometrical series solution provides a closer match to the moisture profiles simulated with the Crank-Nicolson’s finite difference model for linear diffusion equation.

2. The simulated moisture profiles are observed to remain concave upwards initially and become linear at later stages for the linear governing model. Although this pattern closely conforms to the trigonometrical series solution, it does not match the experimentally observed distribution.

3. The exponential hydraulic diffusivity function gives a better simulation of experimental observations in terms of the shape of the moisture distribution and its associated characteristics i.e. moisture content and penetration depth.

4. The magnitude of constant diffusivity models matches the non-linear hydraulic diffusivity values at about 80% and 70% saturation levels for fired clay brick and OPC-lime-sand mortar respectively. This would lead to the over estimation of moisture intrusion at lower and under estimation at higher saturation levels when using a linear model.

5. The study also reveals that, that the non-linear model performs better in the case of fired clay brick than for the OPC-lime-sand mortar. The reason may be attributed to the self-sealing effect typical of cementitious systems.

ACKNOWLEDGMENTS

The authors acknowledge the ECR grant (No. ECR/2016/001240) provided by SERB, DST for the project “Modelling of hydraulic diffusivity and its application in the FE-simulation of moisture transport in concrete for assessing corrosion risk.”

REFERENCES

1. KUNZEL H M, Simultaneous heat and moisture transport in building components - One- and two-dimensional calculation using simple parameters, IRB-Verlag Stuttgart Jan 1995.

2. HALL C AND HOFF W D, Water transport in brick, stone and concrete, Text Book. CRC Press.
3. PEL L, HUININK H AND KOPINGA K, Salt transport and crystallization in porous building materials, Magnetic Resonance Imaging, April 2003, Vol 21(3/4), pp 317-20.
4. SARKAR K AND BHATTACHARJEE B, The role of moisture in degrading concrete, National Conference on Emerging Trends in Civil Engineering, 2016, pp 134-142.
5. RUCKER-GRAMM P AND BEDDOE R E, Effect of the moisture content of concrete on water uptake, Cement and Concrete Research, Jan 2010, Vol 40 (1), pp 102-108.
6. WANG Y AND YUNPING X, The effect of temperature on moisture transport in concrete, Materials, Aug 2017, Vol 10 (8), pp 926.
7. MUKHOPADHYAYA P, KUMARAN K, NORMANDIN N AND GOUDREAU P, Effect of surface temperature on water absorption coefficient of building materials, Journal of Thermal Envelope and Building Science, October 2002, Vol 26, pp 179-195.
8. KARAGIANNIS N, KAROGLOU M, BAKOLAS A AND MOROPOULOU A, Building materials capillary rise coefficient: concepts, determination and parameters involved, New approaches to building pathology and durability, 2016, Springer, Singapore, pp 27-44.
9. ASTM: C1585 – 13. Standard test method for measurement of rate of absorption of water by hydraulic-cement concretes.
10. BS: 1881(Part 208). Determination of Initial Surface Absorption of Concrete (ISAT). 1996.
11. SICAKOVAA A, DRAGANOVSKAA M AND KOVACA M, Water absorption coefficient as a performance characteristic of building mixes containing fine particles of selected recycled materials, Procedia Engineering, Jan 2017, Vol 180, pp 1256-65.
12. LOCKINGTON D, PARLANGE J Y AND DUX1 P, Sorptivity and the estimation of water penetration into unsaturated concrete, Materials and Structures/Matériaux et Constructions, Vol 32, June 1999, pp 342-347.
13. KOPINGA K AND PEL L, One-dimensional scanning of moisture in porous materials with NMR, Review of Scientific Instruments, 1994, Vol 65 (12), pp 3673-3681.
14. NIZOVTSEV M I, STANKUS S V, STERLYAGOV A N, TEREKHOV V I, AND KHAIRULIN RA, Determination of moisture diffusivity in porous materials using Gamma-Method, International Journal of Heat and Mass Transfer, Aug 2008, Vol 51, pp 4161–4167.
15. CHARLES J K, VINCENT C J AND CHRISTOPHER M B, Time-Domain Reflectometry of water content in Portland cement concrete, US Army Corps of Engineers Cold Regions Research & Engineering Laboratory, November 1997, Special Report 97-27.
16. GOUAL M S, BARQUIN D E, BENMALEK M L, BALIC A AND QUEANEUDEC M, Estimation of the capillary transport coefficient of clayey aerated concrete using a gravimetric technique, Cement and Concrete Research, July 2000, Vol 30, pp 1559-1563.
17. PEL L, Moisture transport in porous building materials, Ph.D. Thesis, Technische Universiteit Eindhoven, Netherlands 1995.
18. HALL C, Water sorptivity of mortars and concretes: a review, Magazine of Concrete Research, June 1989, Vol 41 No. 147, pp 5 1-61.
19. CRANK J, The mathematics of diffusion, Oxford Science, New York, 1989.
20. GARBALINSKA L, Measurements of the mass diffusivity in cement mortar: use of initial rates of water absorption, International Journal of Heat and Mass Transfer, March 2002, Vol 45, pp 1353-1357.

21. JANETTI A M B AND WAGNER P, Analytical model for the moisture absorption in capillary active building materials, Building and Environment, Sep 2017, Vol 126, pp 98-106.
22. KUMARAN M K, Moisture diffusivity of building materials from water absorption measurements, J. Thermal ENV. & BLDG. SCI. Vol 22, April 1999, pp 349-355.
23. WILSON M A, CARTER M A AND HOFF W D, British standard and RILEM water absorption test: A critical value, Materials and Structures, Vol 32, October 1999, pp 571-578.
24. HANUMANTHU K AND SARKAR K, Numerical simulation of one-dimensional capillary water absorption in porous building materials, International Conference on Advances in Construction Materials and Structures, March 2018.
25. GASPARIN S, BERGER J, DUTYKH D AND MENDES N, Stable explicit schemes for simulation of non-linear moisture transfer in porous materials, Journal of International Building Performance Simulation Association (IBPSA), March 2018, Vol 11(2), pp.129-144.